SURFACE VEHICLE INFORMATION REPORT

J1975™ NOV2024

Issued 1991-06
Revised 1997-11
Reaffirmed 2024-11

Superseding J1975 NOV1997

Case Hardenability of Carburized Steels

RATIONALE

SAE J1975 has been reaffirmed to comply with the SAE Five-Year Review policy.

1. ***Scope—***This SAE Information Report summarizes the characteristics of carburized steels and factors involved in controlling hardness, microstructure, and residual stress. Methods of determining case hardenability are reviewed, as well as methods to test for freedom from non-martensitic structures in the carburized case. Factors influencing case hardenability are also reviewed. Methods of predicting case hardenability are included, with examples of calculations for several standard carburizing steels. A bibliography is included in 2.2. The references provide more detailed information on the topics discussed in this document.

2. ***References***

2.1 Applicable Publications—The following publications form a part of this specification to the extent specified herein. Unless otherwise indicated, the latest issue of SAE publications shall apply.

2.1.1 SAE PUBLICATIONS—Available from SAE, 400 Commonwealth Drive, Warrendale, PA 15096-0001.

SAE J403—Chemical Compositions of SAE Carbon Steels
SAE J404—Chemical Compositions of SAE Alloy Steels
SAE J406—Methods of Determining Hardenability of Steels
SAE J417—Hardness Tests and Hardness Number Conversions
SAE J1268—Hardenability Bands for Carbon and Alloy H Steels

2.2 Other Publications

1. R.F. Thomson, "Summary," *Fatigue Durability of Carburized Steel*, ASM International, Metals Park, Ohio, 1957, p. 110.
2. D.H. Breen, "Fundamentals of Gear Stress/Strength Relationships—Materials," SAE Technical Paper 841083, 1984.
3. J.M. Hodge and M.A. Orehoski, "Relationship Between Hardenability and Percentage of Martensite in Some Low Alloy Steels," Trans. AIME, 1946, Vol. 167, pp. 627–642.
4. M. Atkins, *Atlas of Continuous Cooling Transformation Diagrams for Engineering Steels*, ASM International and British Steel Corporation, 1980.
5. A. Rose and H. Hougardy, *Atlas zur Waermebehandlung der Stahle*, V.2, 1972, Max-Planck-Institut fuer Eisenforschung; Verlag Stahleisen m.b.H., P.O. Box 8229, D-4000, Dusseldorf, West Germany. Summarized in English by Rose and Hougardy in “Transformation Characteristics and Hardenability of Carburizing Steels,” in the proceedings of the Symposium Transformation and Hardenability in Steels, Climax Molybdenum Co., 1967, pages 155-167.

TO PLACE A DOCUMENT ORDER: **Tel: 877-606-7323 (inside USA and Canada)**
Tel: +1 724-776-4970 (outside USA)
Fax: 724-776-0790
Email: CustomerService@sae.org
SAE WEB ADDRESS: **http://www.sae.org**

For more information on this standard, visit
https://www.sae.org/standards/content/J1975_202411/

6. C.A. Siebert, D.V. Doane and D.H. Breen, *The Hardenability of Steels—Concepts, Metallurgical Influences, and Industrial Applications*, ASM International, 1977, pp. 163–176.
7. "Modern carburized nickel alloy steels," Reference Book No. 11005, Nickel Development Institute, Toronto, Ontario, Canada M5H 3S6, 1990, pages 19-22.
8. A.E. Gurley and C.R. Hannewald, "Development and Applications of Iso-Hardness Diagrams," Metal Treating, V. 7, May-June 1956, p. 2.
9. J. A. Halgren and E.A. Solecki, "Case Hardenability of SAE 4028, 8620, 4620 and 4815 Steels," SAE Technical Paper 149A, 1960.
10. Atlas, *Hardenability of Carburized Steels*, Climax Molybdenum Co., 1960.
11. D.E. Diesburg, C. Kim and W. Fairhurst, "Microstructure and Residual Stress Effects on the Fracture of Case-Hardened Steels," Proceedings of *Heat Treatment '81*, The Metals Society, London, September, 1981.
12. R.F. Kern, Metal Progress, Oct. 1972, p. 172.
13. G.T. Eldis and Y.E. Smith, "Effect of Composition on Distance to First Bainite in Carburized Steels," Journal of Heat Treating, V. 2, No. 1, June 1981, pp. 62–72.
14. I.R. Kramer, S. Siegel and J.G. Brooks, "Factors for the Calculation of Hardenability," Trans. AIME, 1946, Vol. 167, p. 670.
15. C.F. Jatczak, "Hardenability in High Carbon Steels," Met. Trans., 1973, V. 4, p. 2272.
16. "New CCT Diagrams for Carburizing Steels," Molybdenum Mosaic, 1987, V. 10, No. 1, AMAX Metal Products, Bridgeville, PA, p. 11.
17. D.V. Doane, "Softening High Hardenability Steels for Machining and Cold Forming," Journal of Heat Treating, V. 6, No. 2, 1988, pp. 97–109.
18. R.J. Love, H.C. Allsopp and A.T. Weare, "The Influence of Carburizing Conditions and Heat Treatment on the Bending Fatigue Strength and Impact Strength of Gears Made from EN352 Steel," MIRA Report No. 19.59/7.
19. J.A. Burnett, "Prediction of Stresses Generated During the Heat Treating of Case Carburized Parts," *Residual Stresses for Designers and Metallurgists*, ASM International, 1981, pp. 51–69.
20. C. Kim, D.E. Diesburg and G.T. Eldis, "Effect of Residual Stress on Fatigue Fracture of Case-Hardened Steels—An Analytical Model," *Residual Stress Effects in Fatigue*, ASTM Special Technical Publication 776, 1982, pp. 224–234.

3. ***General—***The typical carburized steel component can be modeled as a composite material with a high-hardness, carbon-rich surface layer on a lower carbon base that is lower in hardness but higher in toughness. The continuous nature of the transition between the high-carbon case and the low-carbon core, combined with the sequence of transformation events occurring throughout the component during quenching result in the development of a microstructural gradient and a favorable residual stress profile. These factors define the overall fatigue and fracture properties of the carburized component.

Failure modes of carburized components influence the choice of case depth and microstructure. To illustrate the nature of the stresses developed in a carburized component, and how they can be effectively used, Figure 1 shows the stresses in a carburized bar subjected to bending fatigue [1].[1] In this situation, the applied stress is highest at the surface and zero at the centerline. The hardness gradient of the carburized and hardened bar indicates the probable gradient in endurance limit (or fatigue limit) which is highest at the surface, and drops through the case-core interface to the lower fatigue limit of the core.

1. Numbers in brackets are references cited in 2.2.

During quenching, the core material transforms first because its lower carbon content has a higher martensite-start temperature. The case material transforms somewhat later because its higher carbon content has a lower martensite-start temperature. Since the strength of the core resists the expansion of the case during its martensite transformation, compressive stresses develop in the case that are balanced by tensile stresses in the core. These residual stresses (curve A) add to, or subtract from, the inherent microstructural strength (curve B), resulting in the net effective fatigue limit (or endurance limit) shown by the dashed curve. Note that in this properly designed and loaded beam, the effective fatigue limit level is always greater than the applied stress. The diagram is over-simplified, of course, to demonstrate the principles involved.

Breen has discussed modes of failure in gears [2] and showed that the applied stresses at the root of the tooth decrease nonlinearly with depth. The high stress level at the surface is a result of the cantilever loading of the gear tooth, intensified by the stress concentration caused by the root radius and surface finish. Thus, for a carburized gear, it is quite important that the effective fatigue limit be as high as possible at the surface.

For failure at and below the contact or pitch line of a gear tooth, the applied stress curve is yet a different shape, as described in Breen's article [2], and illustrated in Figure 2. Hertzian stresses are greatest below the surface, the depth depending on the profile of the surfaces in contact. If the net fatigue limit curve, the critical strength curve B shown in the figure, coincides with the applied stress curve A at some depth X below the surface, e.g., at the case-core interface, then subcase (spalling) fatigue can occur. This failure mode emphasizes the need to provide adequate case depth and optimum microstructure at all carbon levels.

The ratio of the volume (or cross-sectional area) of case to core defines the magnitude of compressive stress at the surface. Thus, for a given part, the magnitude of the compressive stress in the case tends to decrease as the case depth increases. When the design is correct, the critical shear strength will remain above the applied stress curve.

3.1 Hardness versus Carbon Content—For a given carbon level there is a systematic relationship between hardness and structure in hardened steel, as shown in Figure 3, from the work of Hodge and Orehoski [3]. The curves not only show the differences due to microstructure, but also the variability in measurements. The spread in hardness at 99.9% martensite is due primarily to measurement errors; the greater spread at 50% martensite is attributable to the variability in the non-martensitic structure. Breen [2] has stated that to resist fatigue failure due to cyclic bending stresses at the root fillet of gears, the optimum case structure is a mixture of high carbon martensite and retained austenite, with enough martensite to assure a hardness of at least 57 HRC. The microstructure in the core should comprise only martensite and bainite. For most alloy carburizing steels, transformation to at least 50% martensite assures that the balance of the structure is bainite [4,5].

To maintain high case hardness, retained austenite must be restricted. Data from Rose and Hougardy [5] on microstructure and hardness of several carburized steels show that alloy content and alloy interactions influence the range of case carbon contents within which a suitable hardness and a martensite/austenite microstructure can be achieved.

3.2 Hardenability—A certain minimum hardenability is necessary to develop the required strength in a carburized part. The hardenability of the base composition governs the capability of developing high strength martensite in the core and in the medium carbon portion of the case. Hardenability in the high carbon region controls the capability of a steel to develop sufficient hardness and an appropriate microstructure at the case surface. The conventional Jominy end-quench test can provide much of the needed information, if case hardenability is considered as well as base, or core, hardenability.

For certain applications, shallow carburized cases may be employed to improve wear resistance under light to moderate load conditions. For such applications, high surface hardness is the important criterion. A fully martensitic structure at the surface provides highest hardness and best resistance to wear. Section size dictates the cooling rate that can be achieved at the surface, especially in parts which are oil quenched (Figure 7 of SAE J406). Cooling rate, expressed as distance from the quenched end of the Jominy hardenability bar, can define the hardenability required.

Hardenability requirements for carburized components are discussed in some detail in an ASM monograph [6], including consideration of section size in terms of "Jominy equivalent," carbon gradient, and surface oxidation. An example uses a gear to demonstrate the engineering approach to steel selection, and the steps involved in reaching a cost-effective choice of steel which meets design requirements. Processing requirements are also included.

4. Methods of Determining Case Hardenability—The end-quench method for determining hardenability is described in SAE J406. The method has been used to determine case as well as core hardenability of carburized steels. Figure 4 shows the core and case hardenability of a heat of SAE 4620 steel, containing nominally 0.2% C, 0.6% Mn, 1.8% Ni, and 0.25% Mo. A common criterion for evaluating the hardenability of a steel is the "ideal critical diameter, D_I." It is defined as the diameter of a bar which exhibits an acceptable microstructure when subjected to an "ideal" quench (a quench of infinite severity, defined in more detail in [6]). For carbon contents in the core and transition regions of a carburized steel, a microstructure of 50% martensite, balance bainite, is often chosen. This microstructure is characteristic of that found in the inflection region of the hardenability curve. This "50% martensite" criterion is indicated by the dashed line in Figure 4, and relates to the D_I for each carbon level. In the carburized case, however, a microstructure containing at least 90% martensite and retained austenite is considered necessary to resist fatigue failure. This "90% martensite" criterion is indicated by another dashed line in Figure 4, and relates to the D_I for case hardenability.

4.1 Jominy End-Quench Test—The test can be used to determine hardness at various carbon levels in the carburized case, as a function of cooling rate, expressed as the distance from the quenched end of the test bar. Figure 4 is one example. The method for determining case hardenability from Jominy end-quench bars is described in detail in Appendix A. Data showing case hardenability can be found in several references [7–10] presented either as standard hardenability curves or as isohardness diagrams.

4.2 Distance to First Appearance of Bainite in the Carburized Case—Data suggest that the as-quenched microstructure must be substantially free from bainite or pearlite to obtain the greatest resistance to impact [11]. The presence of very small amounts of bainite in the case has also been reported to reduce fatigue resistance [12]. Eldis and Smith reported the results of a detailed study of the occurrence of bainite in carburized end-quench hardenability specimens [13]. In the study, specimens of 81 alloys were carburized at 925 °C (1700 °F), cooled to 845 °C (1550 °F) and end-quenched. Companion bars were carburized to provide carbon gradient data. Flats were ground on the bars to a depth corresponding to 0.9% carbon in the case and hardness profiles were determined. Those flats were then metallographically polished, etched, and examined using quantitative metallographic techniques to determine the amount of bainite as a function of distance from the quenched end of the bar. The data for percent bainite were plotted and extrapolated to determine the "distance to first (appearance) of bainite" (DFB). Figure 5 shows a schematic diagram of the test technique.

Figure 6 shows data obtained for three steels, plotted on standard hardenability coordinates. It clearly illustrates that one cannot detect the presence of small amounts of bainite from hardness data. The results of the investigation [13] were subjected to multiple regression analysis to develop an empirical relationship for predicting DFB from composition. The regression equations appear below, and are valid at the 0.9% C level in the case for steels containing 0.5 to 1.1% Mn, 0 to 1.5% Ni, 0 to 1.0% Cr, and 0 to 0.5% Mo. Alloy contents are entered in weight percent:

$$\text{DFB (in millimeters from the quenched end)} = 54.7Mo^2 + 6.4Cr^2 - 76.1MoNi + 118.8MnMoNi + 106.1\,MnMoCr + 15.5MnNiCr + 52.9MoNiCr + 1.18 \quad \text{(Eq. 1)}$$

or

$$\text{DFB (in sixteenths of an inch from the quenched end)} = 34.5Mo^2 + 4.0Cr^2 - 47.9MoNi + 74.8MnMoNi + 66.9MnMoCr + 9.8MnNiCr + 33.3MoNiCr + 0.7 \quad \text{(Eq. 2)}$$

It is important to recognize that alloy interactions influence the presence of bainite in the carburized case. One should check these interactions when modifying a carburizing steel composition. The regression equations provide a convenient method of predicting the effect of changes in composition on DFB. They also can aid in the establishment of a minimum alloy content to assure a bainite-free microstructure in the carburized case.

5. Calculating Case Hardenability—D_I can be calculated using the general equation:

$$D_I = D_I^o(MF_{Si})(MN_{Mn})(MF_{Ni})(MF_{Cr})(MF_{Mo}) \quad \text{(Eq. 3)}$$

where:

D_I^o is the base D_I for carbon (and grain size), as shown in Figure 7, and
MF_x is the multiplying factor for each alloying element, taken from a table or graph, such as Figure 8, or a specialized slide rule.

D_I can also be calculated using computer programs, which may include alloy interaction effects.

Core hardenability (expressed as 50% martensite D_I), case hardenability (expressed as 90% martensite D_I), and distance to first appearance of bainite (DFB) were calculated for several standard carburizing steels. For core hardenability, the method given in the Appendix of SAE J406 was used. The methods described in this document were used to calculate case D_I and DFB. For each steel, the midrange composition was selected for calculation purposes (assuming no residual elements), and 0.9% carbon was chosen for case D_I calculations (assuming a quench temperature of 925 °C, 1700 °F). The results are shown in Table 1. It is evident that one cannot assume that case hardenability or freedom from bainite will be proportional to core hardenability. The materials engineer must know the requirements for both case and core hardenability to provide a steel that can adequately meet both of these requirements.

5.1 Factors Influencing Case Hardenability—As shown in Figure 4, carbon is exceedingly influential in increasing both hardness and hardenability. This is also evident from data on the effect of carbon on hardenability multiplying factors (or D_I) as shown in Figure 7. Note the additional influence of austenitizing temperature, and the fact that there is an optimum carbon content at which the carbon effect is at a maximum.

The apparent loss of hardenability at carbon levels above 0.8% carbon at normal austenitizing temperatures is due to the formation of alloy carbides. At normal austenitizing temperatures these alloy carbides that form above 0.8% carbon do not fully redissolve, thus the benefit of the alloy elements tied up as carbides is lost. The hardenability effect of these alloy elements could be recovered if a higher austenitizing temperature was used. But such temperatures are not usually recommended for standard carburizing steels due to the adverse effects on grain growth, cracking, and distortion.

The curves in Figure 7 for 0.2 to 0.7% carbon are those of Kramer [14]; the curves for 0.6 to 1.1% carbon are those developed by Jatczak [15]. Alloy multiplying factors developed by Jatczak for carburized steels are shown in Figure 8. The alloy factors were developed for microstructures containing less than 10% pearlite or bainite.

TABLE 1—CORE AND CASE HARDENABILITY COMPARISON (DATA IN MILLIMETERS, WITH INCHES IN PARENTHESES)

Steel Grade[1]	Mid-range Composition wt. % C	Mid-range Composition wt. % Mn	Mid-range Composition wt. % Si	Mid-range Composition wt. % Cr	Mid-range Composition wt. % Ni	Mid-range Composition wt. % Mo	Core D_I [50% M]	Core D_I [90% M]	D_{FB} [J_D in 16ths]
1018	0.18	0.75	0.25	—	—	—	10	48	<1.5
							(0.4)	(1.9)	(<1)
4028H	0.27	0.80	0.25	—	—	0.25	28	86	5
							(1.1)	(3.4)	(3)
4118H	0.20	0.80	0.25	0.50	—	0.11	33	105	8
							(1.3)	(4.2)	(5)
4120H	0.20	1.05	0.25	0.50	—	0.18	46	145	14
							(1.8)	(5.8)	(9)
4121	0.21	0.88	0.25	0.55	—	0.25	48	157	19
							(1.9)	(6.2)	(12)
4130H	0.30	0.50	0.25	1.00	—	0.20	66	145	21
							(2.6)	(5.7)	(13)
4320H	0.20	0.55	0.25	0.50	1.75	0.25	56	225	27[2]
							(2.2)	(8.8)	(17[2])
5120H	0.20	0.80	0.25	0.80	—	—	33	100	5
							(1.3)	(4.0)	(3)
8620H	0.20	0.80	0.25	0.50	0.55	0.20	48	150	22
							(1.9)	(6.0)	(14)
8720H	0.20	0.80	0.25	0.50	0.55	0.25	51	175	27
							(2.0)	(6.9)	(17)
8822H	0.22	0.88	0.25	0.50	0.55	0.35	71	215	40
							(2.8)	(8.5)	(25)

1. SAE grades, from composition ranges given in SAE J403 (for carbon steel 1018), SAE J404 (for alloy steel 4121) and SAE J1268 (for H steels).
2. Note that nickel content falls outside the 0 to 1.5% Ni range of steels used in developing the regression equation.

6. Continuous-Cooling Transformation (CCT) Diagrams—Carbon content and microstructure resulting from transformation during heat treatment exert control over the properties of carburized steel. As shown in previous sections, the results of Jominy end-quench tests provide good hardness data, but only indirectly indicate microstructure. A more direct way of defining microstructure as a function of cooling characteristics is the continuous-cooling transformation (CCT) diagram. A partial CCT diagram for SAE 4815H steel is shown in Figure 9, from [16]. Note the time-temperature regions in which ferrite, pearlite, bainite, and martensite occur during cooling the steel from the austenitizing temperature at a series of controlled rates. Cooling at rates faster than those which intersect a region of higher temperature transformation will result in martensitic structures at room temperature.

In developing the CCT diagrams, hardness data are obtained from the as-cooled specimens. Vickers hardness values (using 10 kg load) are shown in circles at the end of the cooling curves. Cooling curves which intersect regions of ferrite, pearlite, or bainite formation show hardness values less than the maximum achieved with a completely martensitic structure. CCT diagrams are usually developed over a wide range of cooling rates, and thus can be used in the development of annealing heat treatments [17] to obtain specific hardness values or microstructures.

Diesburg and others [11] have pointed out that large variations in resistance to impact can be at least partially explained by the presence of bainite at the subsurface carbon levels in the carburized case. Therefore, data on the effect of carbon on transformation characteristics are useful in determining how to prevent the occurrence of undesirable microstructures.

CCT diagrams are available for several steels having the same base composition, but varying carbon contents corresponding to carbon levels attained during carburizing [4,5]. Figure 10 shows partial CCT diagrams (reported in the Diesburg reference [11]) for three such steel base compositions, and provides some insight into the transformation behavior during cooling after carburizing. Shown in the figure are transformation-start curves for various carbon levels, plus a range of cooling conditions encountered in parts of moderate section size. At the left end of each curve is the hardness (HV10) of the structure, predominantly martensite, formed at fast cooling rates. Steels of higher hardenability are required to eliminate formation of pearlite and bainite at intermediate carbon levels in the case. Note that with SAE 4620 steel, one can expect bainite near the carburized surface (the 0.8% C curve) at cooling rates encountered in quenching even moderate section sizes. Increasing the alloy content slightly can avoid such bainite transformation (as with the Mo-modified 4600 steel).

7. Related Parameters—In addition to hardness and microstructure, one needs to consider the effects of case depth and residual stress on the properties of carburized components. Case depth and case properties (hardness and residual stresses) can be developed to provide critical strength levels greater than the applied stress at all locations in the carburized part. The magnitude of residual stress, and thus the net effective bending fatigue strength (fatigue limit) of carburized steel, is influenced by case depth.

7.1 Case Depth—Experience has shown that once a case depth has been attained that is sufficient to (a) prevent case crushing, and (b) provide adequate fatigue life, there is nothing to be gained by further increasing case depth. In fact, some British work [18] shows that over-carburizing can decrease the fatigue limit of a part. That work also shows that higher fatigue limits can be achieved at higher quenching temperatures.

7.2 Residual Stress—The magnitude of residual stress is dependent on processing variables, such as case depth, but is also dependent on material variables, such as hardenability. Burnett [19] developed a method to predict the stresses generated during heat treatment of carburized parts. The method was based on extensive experimental data on thermal gradients, carbon gradients, and phase transformations, plus a knowledge of elastic-plastic behavior as a function of carbon content and temperature.

Kim and others [20] have shown that fatigue crack initiation and propagation in carburized steels are significantly delayed in the presence of residual compressive stresses. They also point out that surface oxidation can counteract the beneficial effect of residual stress.

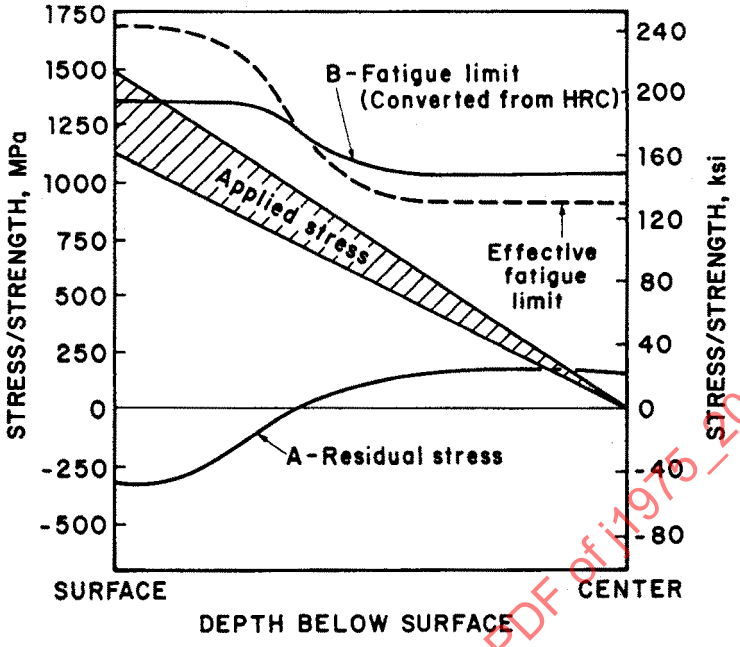

FIGURE 1—SCHEMATIC DIAGRAM OF STRESSES IN A CARBURIZED BAR, LOADED IN SIMPLE BENDING

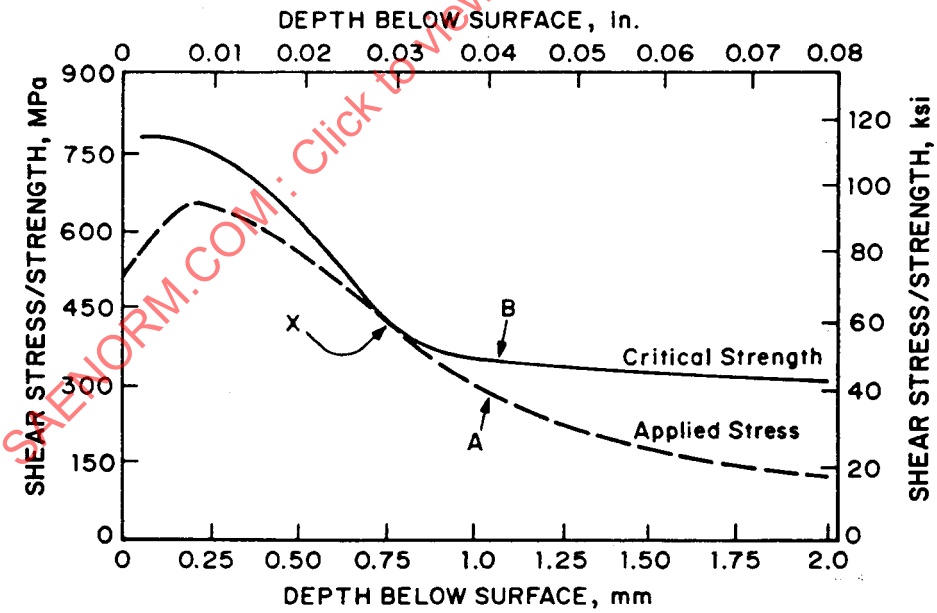

FIGURE 2—APPLIED STRESSES AT THE PITCH LINE OF A GEAR TOOTH REACH A MAXIMUM BELOW THE SURFACE AND THEN DECREASE. THE CRITICAL STRENGTH CURVE DEFINES THE NET FATIGUE LIMIT

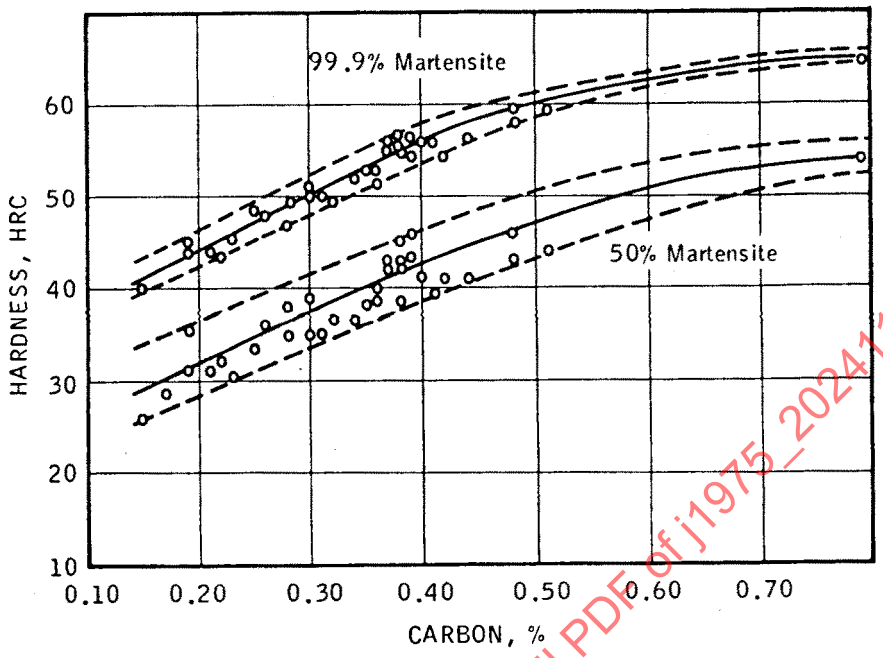

FIGURE 3—HARDNESS OF MARTENSITE PRODUCTS AS A FUNCTION OF CARBON CONTENT

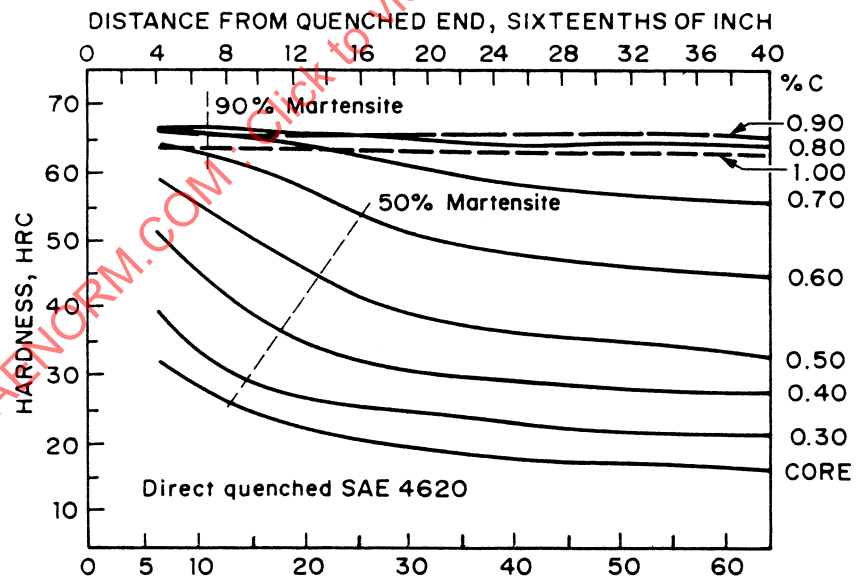

FIGURE 4—CORE AND CASE HARDENABILITY OF A HEAT OF SAE 4620

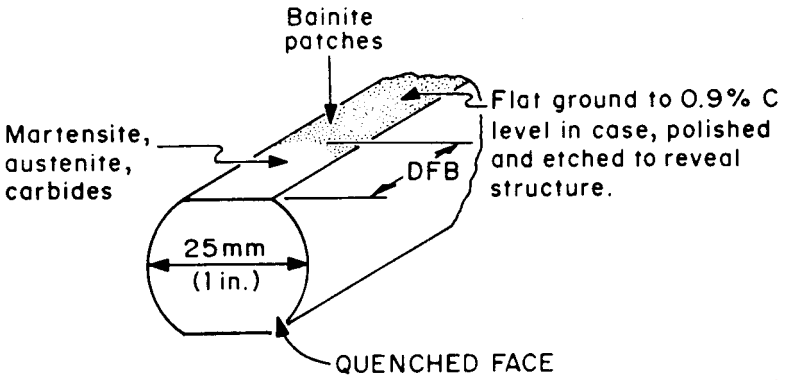

FIGURE 5—SKETCH OF A JOMINY END-QUENCH HARDENABILITY BAR SHOWING THE METHOD USED TO DETERMINE DISTANCE TO FIRST APPEARANCE OF BAINITE (DFB)

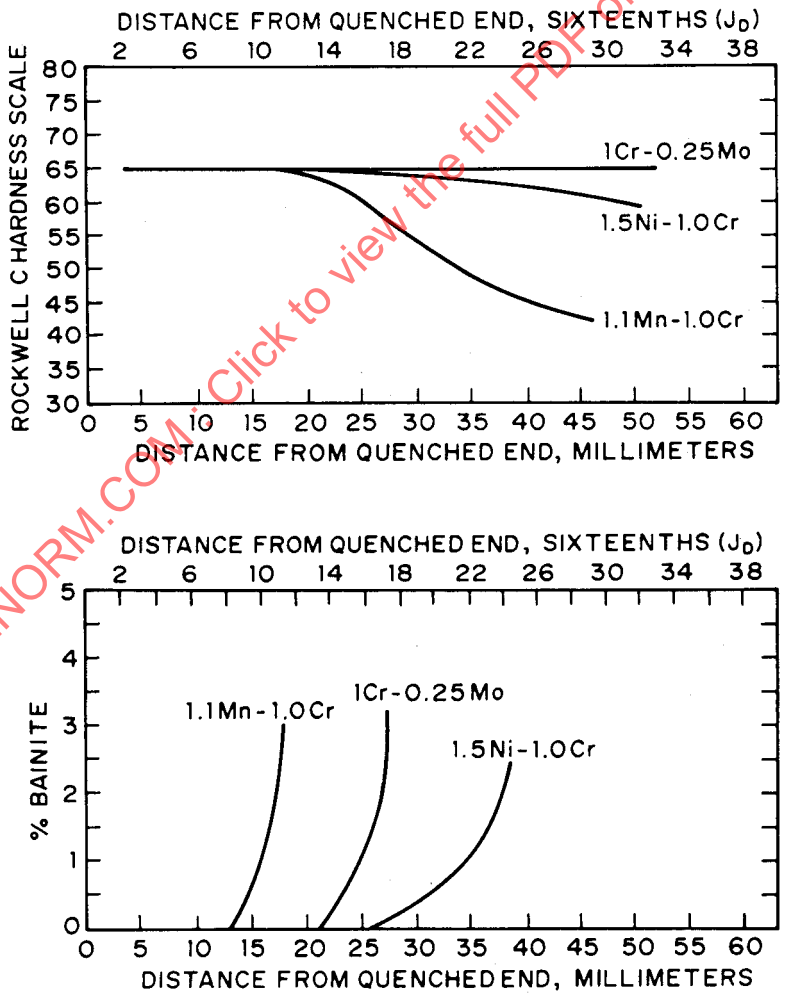

FIGURE 6—CASE HARDENABILITY DATA (UPPER DIAGRAM) AND CORRESPONDING BAINITE PROFILE DATA (LOWER DIAGRAM) FOR THREE STEELS

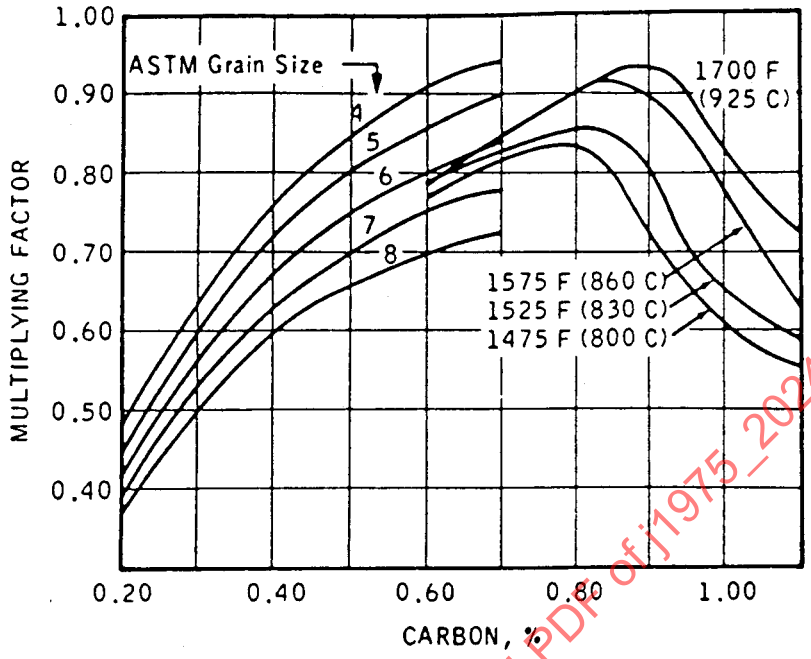

FIGURE 7—MULTIPLYING FACTORS FOR CARBON (D_I^0) IN THE RANGE 0.6 TO 1.1% C AT EACH AUSTENITIZING CONDITION (PLOTTED WITH DATA FOR LOWER CARBON CONTENTS)

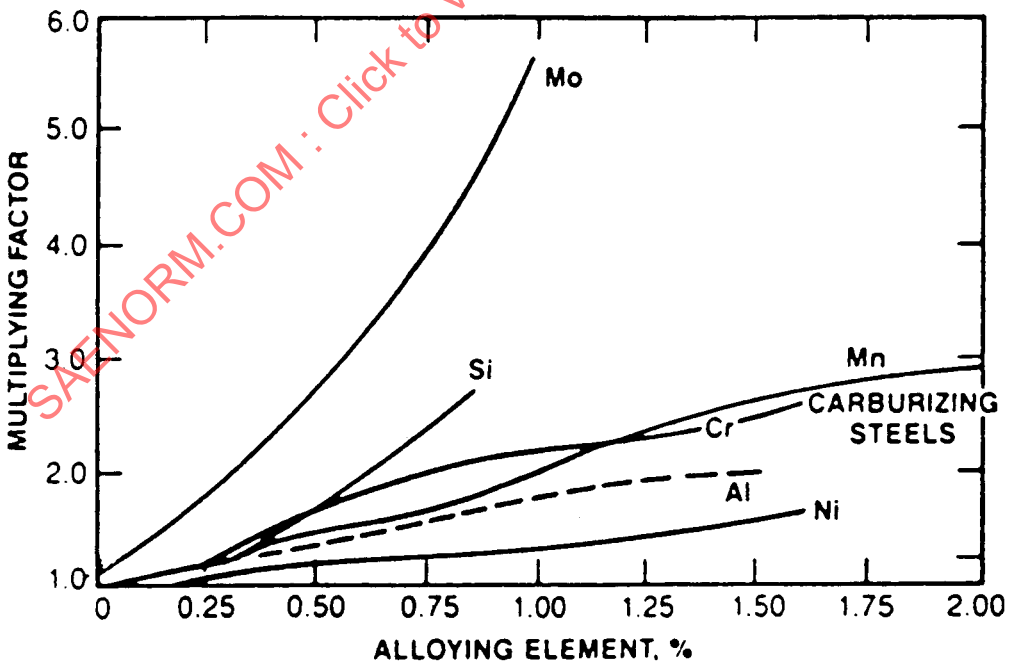

FIGURE 8—HARDENABILITY MULTIPLYING FACTORS FOR ALLOYING ELEMENTS IN THE CARBURIZED CASE (0.6 TO 1.1% C)

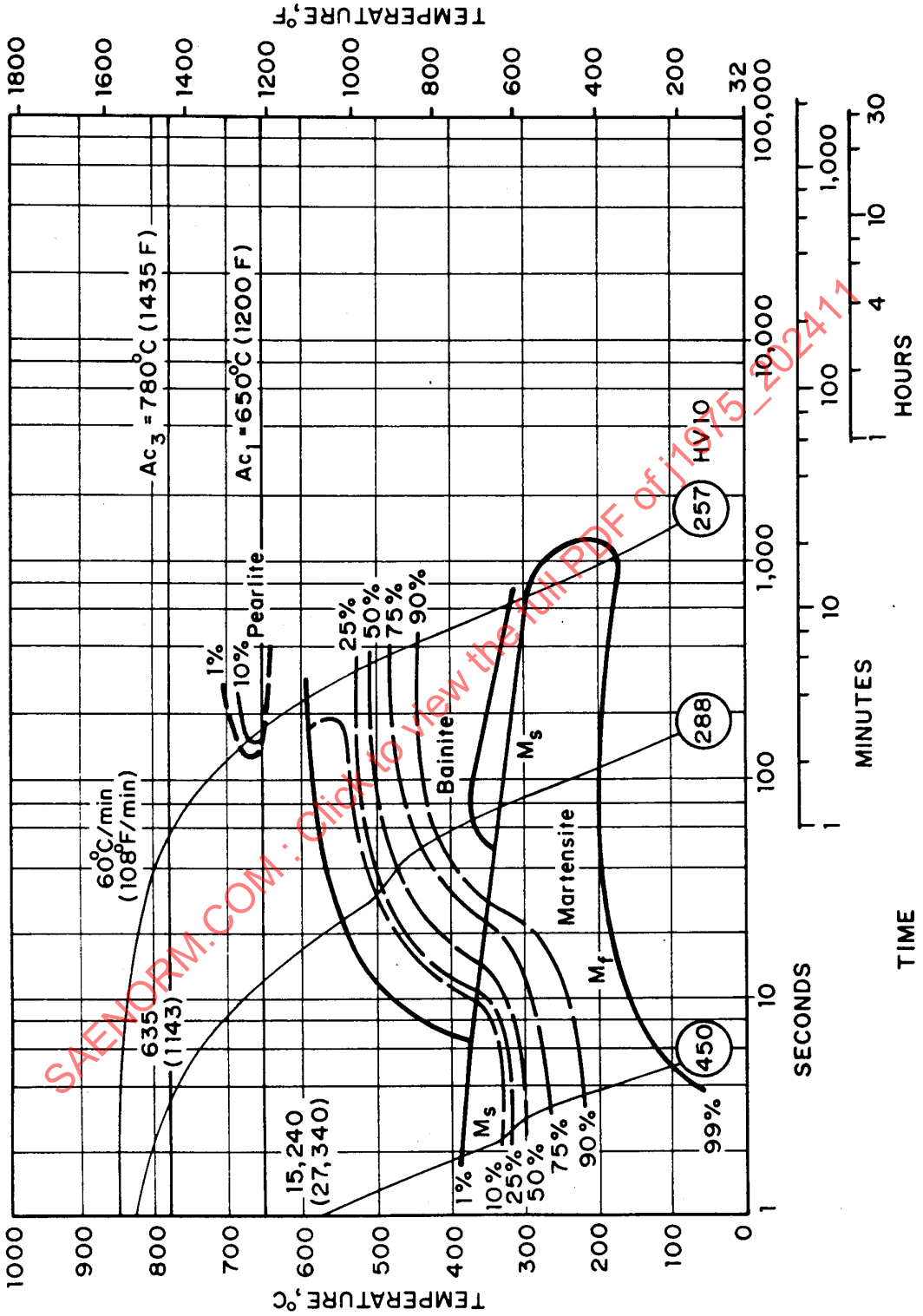

FIGURE 9—CONTINUOUS COOLING TRANSFORMATION (CCT) DIAGRAM FOR SAE J4815H, AUSTENITIZED AT 870 °C (1600 °F). THE STEEL CONTAINED 0.16% C, 0.24% SI, 0.63% MN,3.35% NI, 0.21% CR, AND 0.24% MO.

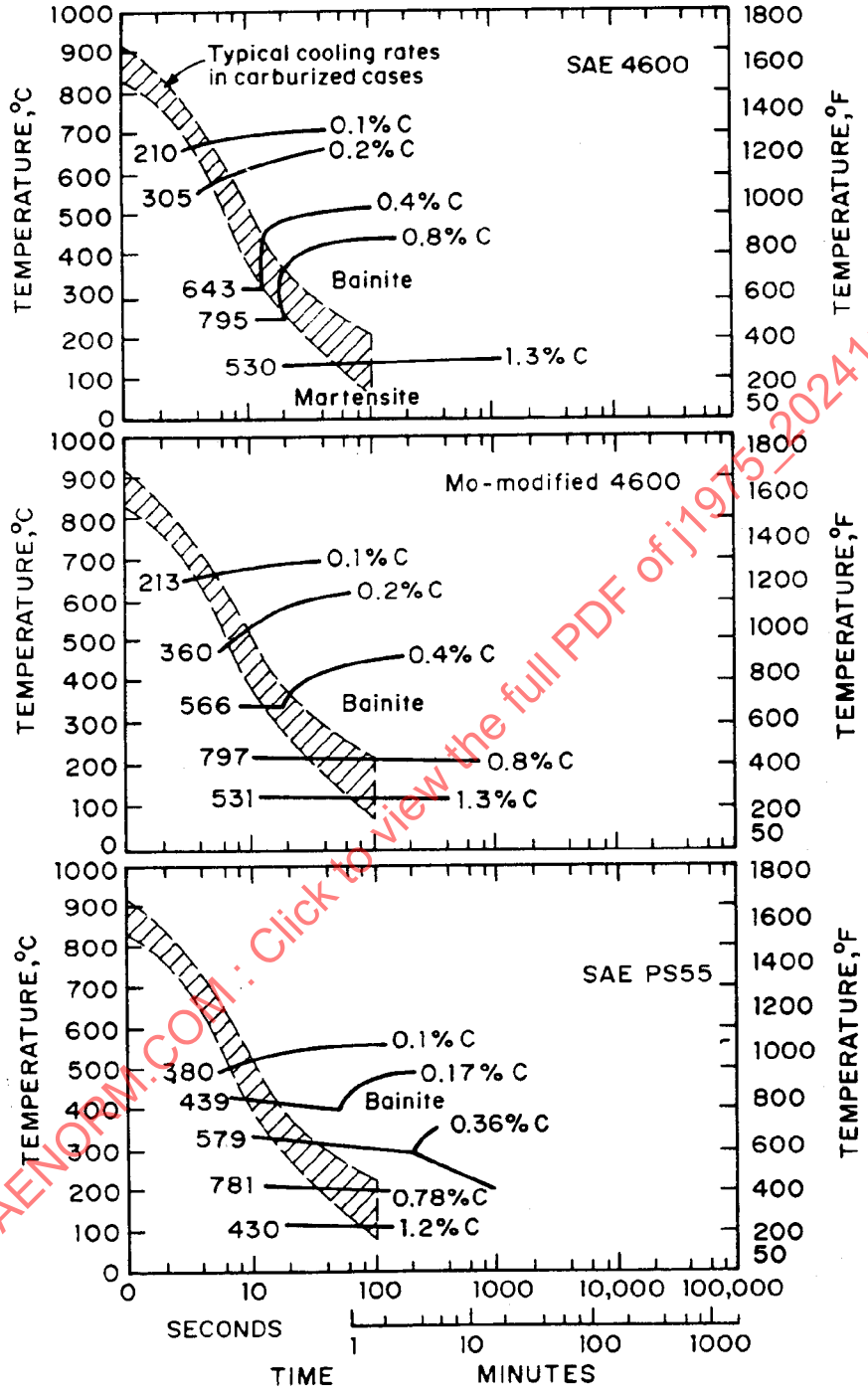

FIGURE 10—PARTIAL CCT DIAGRAMS FOR THREE CARBURIZING STEELS WITH FIVE LEVELS OF CARBON. MARTENSITIC HARDNESS VALUES (HV10), OR HARDNESS OF MARTENSITE-BAINITE AGGREGATE AT LOWEST CARBON CONTENTS, ARE SHOWN FOR EACH CARBON LEVEL. ALLOY CONTENTS ARE:

SAE 4600: 0.62% MN, 1.78% NI, 0.25% MO

MODIFIED 4600: 0.58% MN, 1.81% NI, 0.47% MO

SAE PS55: 0.89% MN, 1.74% NI, 0.60% CR, 0.74% MO